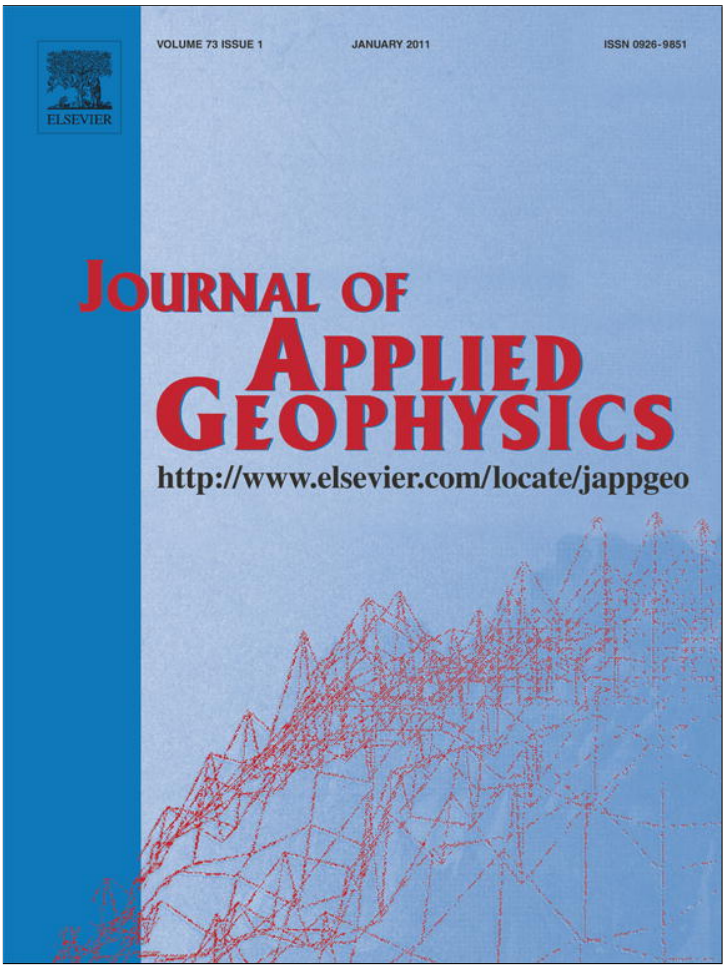

(This is a sample cover image for this issue. The actual cover is not yet available at this time.)

Journal of Applied Geophysics 74 (2011) 229–235

Contents lists available at ScienceDirect

Journal of Applied Geophysics

journal homepage: www.elsevier.com/locate/jappgeo

Kerogen to oil conversion in source rocks. Pore-pressure build-up and effects on seismic velocities

Giorgia Pinna, José M. Carcione *, Flavio Poletto

[a] Istituto Nazionale di Oceanografia e di Geofisica Sperimentale (OGS), Borgo Grotta Gigante 42c, 34010 Sgonico, Trieste, Italy

ARTICLE INFO

Article history:
Received 13 October 2010
Accepted 25 May 2011
Available online xxxx

Keywords:
Source rock
Seismic velocity
Gassmann equations
Pore pressure
Kerogen–oil conversion

ABSTRACT

The aim of this work is to obtain a model for source rocks relating to kerogen–oil conversion and pore pressure to seismic velocity and anisotropy. The source rock is described by a porous transversely isotropic medium composed of illite/smectite and organic matter. The rock has a very low permeability and pore-pressure build-up occurs. We consider a basin-evolution model with constant sedimentation rate and geothermal gradient. Kerogen–oil conversion starts at a given depth in a volume whose permeability is sufficiently low so that the increase in pressure due to oil generation greatly exceeds the dissipation of pressure by flow. Assuming a first-order kinetic reaction, with a reaction rate satisfying the Arrhenius equation, the kerogen–oil conversion fraction is calculated. Pore-pressure changes affect the dry-rock stiffnesses, which have an influence on seismic velocities. The properties of the kerogen–oil mixture are obtained with the Kuster and Toksöz model, assuming that oil is the inclusion in a kerogen matrix. We use Gassmann's equations generalized to the anisotropic case to obtain the seismic velocities of the source rock as a function of depth, pressure and oil saturation. The procedure is to obtain the dry-rock stiffnesses by assuming a Poisson medium for the mineral material constrained by the physical stability conditions at the calibration confining pressures.

The example considers a sample of the North-Sea Kimmeridge shale. At a given depth, the conversion increases with increasing geothermal gradient and decreasing sedimentation rate, and the porosity increases with depth due to the conversion. As expected, the horizontal velocities are greater than the vertical velocities and the degree of anisotropy increases with depth. The analysis reveals that the vertical P-wave velocity is the main indicator of overpressure.

1. Introduction

Oil can be generated from kerogen-rich source rocks and flow through a carrier bed to a sandstone reservoir rock. Excess pore-fluid pressures are generated when the rate of volume created by the transformation of oil to gas is more rapid than the rate of volume loss by fluid flow. Research conducted by Vernik on petroleum source rocks (Vernik and Nur, 1992; Vernik, 1994, 1995; Vernik and Landis, 1996) indicates that strong velocity anisotropy is associated with the presence of organic matter.

Berg and Gangi (1999) derived a procedure to obtain the conversion of kerogen to oil and the related pressure buildup in a source rock, based on the following assumptions. i) The permeability of the rock is small so that the pore-pressure buildup by the conversion is much faster than its dissipation by pore-fluid flow. ii) The stress state is isotropic and the rock breaks when the pore pressure equals the confining pressure. iii) One reaction rate is required for the conversion. Carcione (2000) used this model to calculate the excess pore pressure as a function of the fraction of kerogen converted to oil. The conversion ratio is computed as a function of time, for a given sedimentation rate and geothermal gradient, using the Arrhenius equation. The excess pore pressure due to the conversion with burial time is derived by balancing mass and volume changes in the pore space (see also Carcione and Gangi, 2000a,b).

Hydrocarbon source rocks are transversely isotropic media composed of organic matter (kerogen and oil) and illite layers. Vernik in his works and Carcione (2000) used Backus averaging to model the seismic velocities. Here, we use a different approach based on Gassmann equations for an anisotropic frame and an isotropic solid pore infill (kerogen–oil) (Ciz and Shapiro, 2007). The effective properties of illite are obtained by assuming an isotropic Poisson medium constrained by the physical stability conditions applied to the elastic constants of the dry frame, which are obtained by inversion of Gassmann's equations. The method is applied to the Kimmeridge shale, from data provided by Vernik (1995). This is the novel part of this work and to our knowledge it is the first application of Gassmann theory and its "fluid-substitution" version (i.e., inverse Gassmann's equation) to describe the properties of organic shales. This is possible to the generalization of the pore-infill to a solid material. Note that the

* Corresponding author. Tel.: +39 40 2140345; fax: +39 40 327521.
E-mail addresses: gpinna@inogs.it (G. Pinna), jcarcione@inogs.it (J.M. Carcione), fpoletto@inogs.it (F. Poletto).

0926-9851/$ – see front matter © 2011 Elsevier B.V. All rights reserved.
doi:10.1016/j.jappgeo.2011.05.006

models based on Backus averaging were developed before the introduction of Ciz and Shapiro (2007) generalization of Gassmann's equations. This new theory, in its isotropic version, has already been used to describe the properties of rocks filled with heavy oil, which has a non-negligible shear modulus (Das and Batzle, 2008).

In the following, K and μ, and ρ indicate bulk and shear moduli, and density, and the indices m, s, o, k and if denote dry matrix (skeleton), solid grain (clay), oil, kerogen and pore infill (kerogen–oil mixture), respectively. Moreover, $c_{IJ}=c_{ijkl}$ is the two-index notation for stiffnesses (Helbig, 1994), s_{IJ} and s_{ijkl} for compliances, and ϕ denotes porosity or proportion of a given material.

2. Kerogen to oil conversion

Firstly, we introduce some useful definitions about the different pressures considered in this work. *Pore pressure*, also known as formation pressure, is the in situ pressure of the fluids in the pores. The pore pressure is equal to the *hydrostatic pressure* when the pore fluids only support the weight of the overlying pore fluids (mainly brine). The *lithostatic* or *confining pressure* is due to the weight of overlying sediments, including the pore fluids. Fractures perpendicular to the minimum compressive stress direction appear for a given pore pressure, typically 70–90% of the confining pressure. In this case, the fluid escapes from the pores and pore pressure decreases. A rock is said to be overpressured when its pore pressure is significantly greater than hydrostatic pressure. The difference between pore pressure and hydrostatic pressure is called *differential pressure*. Acoustic and transport properties of rocks generally depend on *effective pressure*, a combination of pore and confining pressures (e.g., Carcione, 2007). Various physical processes cause anomalous pressures on an underground fluid. The most common causes of overpressure are compaction disequilibrium and cracking, i.e., oil to gas conversion (Carcione and Gangi, 2000a,b).

Let us assume a source rock at depth z. The lithostatic pressure for an average sediment density of $\bar{\rho}$ is equal to $p_c=\bar{\rho}gz$, where g is the acceleration of gravity. On the other hand, the hydrostatic pore pressure is approximately $p_H=\rho_w gz$, where ρ_w is the density of water.

For a constant sediment burial rate, S, and a constant geothermal gradient, G, the temperature variation of a particular sediment volume is

$$T=T_0+Gz,\ z=St, \tag{1}$$

with a surface temperature T_0 at time $t=0$. Typical values of G range from 20 to 30 °C/km, while S may range between 0.02 and 0.5 km/m.y. (m.y. = milion years).

Assume that at time t_i, corresponding to depth z_i, the shale contains kerogen and that the volume is "closed". That is, the permeability is sufficiently low so that the rate of pressure increase due to oil generation greatly exceeds the dissipation of pressure by flow. Pore pressure excess is intended to be above hydrostatic.

2.1. Kerogen–oil generation rate

The mass of convertible kerogen changes with time t at a rate proportional to the mass present. Assuming a first-order kinetic reaction (Luo and Vasseur, 1996; Pepper and Corvi, 1995)

$$\frac{dM_k}{dt}=-r_k(t)M_k(t) \tag{2}$$

or

$$M_k(t)=M_{ki}\ exp\left[-\int_{t_i}^{t} r_k(t)dt\right], \tag{3}$$

where $r_k(t)$ is the reaction rate, $M_k(t)$ is the mass of convertible kerogen at time t and M_{ki} is the initial kerogen mass. The fraction of kerogen converted to oil is $F(t)=[M_{ki}-M_k(t)]/M_{ki}$:

$$F(t)=1-\ exp\left[-\int_{t_i}^{t} r_k(t')dt'\right]\equiv 1-\ exp[-\Phi(t)]. \tag{4}$$

The reaction rate follows the Arrhenius equation (e.g., Luo and Vasseur, 1996)

$$r_k(t)=A\ exp[-E/RT(t)], \tag{5}$$

where E is the kerogen–oil activation energy, $R=1.986$ cal/mol °K is the gas constant, A is the kerogen–oil reaction rate at infinite temperature, and $T(t)$ is the absolute temperature in °K given by

$$T=T_0+Ht,\ H=GS. \tag{6}$$

With this temperature dependence, the integral $\Phi(t)$ becomes

$$\Phi(t)=\int_{t_i}^{t} r_k(t')dt'=\frac{A}{H}\int_{T_i}^{T} exp(-E/RT')dT',\ T_i=T_o+Ht_i \tag{7}$$

or

$$\Phi(t)=\frac{A}{H}\left[T\int_1^{\infty} exp(-Ex/RT)\frac{dx}{x^2}-T_i\int_1^{\infty} exp(-Ex/RT_i)\frac{dx}{x^2}\right]. \tag{8}$$

For values of E/RT greater than 10, the exponential integral can be approximated by Gautschi and Cahill (1964, pp. 248, Table 5.5)

$$\int_1^{\infty} exp(Ex/RT)\frac{dx}{x^2}\cong\frac{exp(-E/RT)}{2+E/RT}, \tag{9}$$

with an error of 1.3% or less. Then, the integral Φ becomes

$$\Phi(T(t))=\frac{A}{H}\left[\frac{T\ exp(-E/RT)}{2+E/RT}-\frac{T_i\ exp(-E/RT_i)}{2+E/RT_i}\right]. \tag{10}$$

2.2. Kerogen to oil conversion versus excess pressure

Excess pore pressure (overpressure) is the main mechanism for oil migration. This phenomenon occurs mainly in low permeability rocks (e.g., compacted shales), where high-density organic matter, such as kerogen, is transformed to less dense fluids (oil and gas), with a rate exceeding the rate of volume loss by flow. In order to obtain a simple formula for computing the excess pore pressure as a function of the volume fraction of kerogen transformed to oil, the following assumptions are made: i) no loss of fluid from the source-rock pore volume (negligible permeability); ii) the compressibilities are independent of pressure and temperature — in particular the pore-space one is that at the initial pore pressure; iii) the initial pore volume contains only convertible kerogen, since water content is very small and is part of the matrix (which contains hydrated smectite in part); iv) negligible conversion of oil to gas; v) the confining pressure is approximately constant during oil generation, i.e., the reaction rate is high enough such that the overburden pressure does not change significantly during the conversion process; and vi) volume changes with temperature are negligible.

As stated by Vernik (1994), horizontal micro-cracks may be initiated and kept open during the conversion process. Our model assumes that permeability is so low that the reaction is local at a microscopic scale. In this sense, the "closed system" assumption can be a rough approximation in some cases, since it may imply an anomalous increase in porosity (approximately 10% in the examples given here). Therefore, a more realistic model should consider

the expulsion of the oil from the rock by considering the shale permeability.

Let us define the excess pore pressure by $\Delta p = p - p_i$, where p_i is the initial pore pressure and p is the pore pressure when a fraction F of kerogen mass has been converted to oil. Since the mass balance is independent of pressure, the amount of converted oil can be expressed as

$$\rho_o V_{oi} = F\rho_k V_{ki}, \tag{11}$$

where ρ_o is the oil density, V_{oi} is the equivalent oil volume (before the conversion) at pressure p_i (see Fig. 1), and V_{ki} is the kerogen volume at p_i. The pore volume at the initial pore pressure is $V_{pi} = V_{ki}$ since there is only kerogen.

The compressibilities of the oil, kerogen and pore space are defined, respectively, as

$$c_o = -\frac{1}{V_o}\frac{dV_o}{dp}, \quad c_k = -\frac{1}{V_k}\frac{dV_k}{dp}, \quad c_p = +\frac{1}{V_p}\frac{dVp}{dp}, \tag{12}$$

where $c_o = (\rho_o v_P^2)^{-1}$ and $c_k = [\rho_k(v_P^2 - 4v_S^2/3)]^{-1}$, with v_P and v_S the P- and S-wave velocities of each medium.

The + sign means that the pore volume increases with increasing pore pressure, since c_p is the compressibility at constant confining pressure (e.g., Carcione, 2007). Integration from p to p_i yields

$$V_o(p) = V_{oi}\exp(-c_o\Delta p),\ V_k(p) = V_{ki}\exp(-c_k\Delta p), V_p(p) = V_{ki}\exp\left(c_p\Delta p\right). \tag{13}$$

Using (11), the oil volume becomes

$$V_o(p) = FDV_{ki}\ exp(-c_o\Delta p), \tag{14}$$

where $D = \rho_k/\rho_o$. Since at pressure p the pore space volume is

$$V_p = (1-F)V_k + V_o, \tag{15}$$

we obtain

$$exp\left(c_p\Delta p\right) = (1-F)\ exp(-c_k\Delta p) + FD\ exp(-c_o\Delta p). \tag{16}$$

Let us consider a typical case. The Kimmeridge shale is located at 3.5 km depth. The lithostatic pressure, for an average overburden density of $\bar{\rho} = 2.4\ g/cm^3$ is equal to $\bar{\rho}gz \simeq 82$ MPa, where g is the acceleration of gravity. On the other hand, the hydrostatic pore pressure is approximately 34 MPa. Thus, the maximum pore pressure change Δp will be from hydrostatic to lithostatic, i.e., nearly 48 MPa (at this excess pressure, the rock may reach the fracturing stage). Since, under these conditions, the arguments in the exponential functions in Eq. (16) are much less than one, these functions can be approximated by $\exp(x) \simeq 1+x$, $x \ll 1$, giving

$$\Delta p = \frac{(D-1)F}{c_p + c_k - F\left[c_p + C_k - D\left(c_p + c_o\right)\right]}. \tag{17}$$

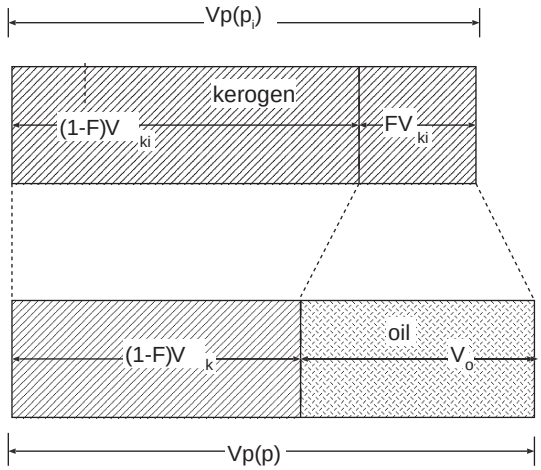

Fig. 1. The variation of the pore, kerogen, and oil volumes with pore pressure: (a) the volume at the initial pore pressure p_i (before any kerogen is converted into oil), and (b) the volumes at the subsequent pore pressure p when a fraction F of kerogen has been converted to oil.

2.2.1. Porosity versus excess pressure

As the pore pressure increases from p_i to p, the pore space volume increases from V_{ki} to $V_{ki}\exp(c_p\Delta p)$, as can be seen in Fig. 1, since kerogen is part of the pore space and this increases due to kerogen–oil conversion. Defining the initial porosity as the initial kerogen proportion K, the porosity increases from this value to $K\exp(c_p\Delta p)$. Then, using Eq. (16), the kerogen and oil proportions can be expressed as a function of pore pressure as

$$\phi_k = K(1-F)\ exp(-c_k\Delta p), \quad \phi_o = KFD\ exp(-c_o\Delta p), \tag{18}$$

respectively. Defining $\phi = \phi_k + \phi_o$ and ϕ_i as the illite proportion, we get

$$\phi_i = 1-\phi = 1-K\exp\left(c_p\Delta p\right). \tag{19}$$

3. Seismic velocities

We consider Gassmann equations for a solid pore infill (kerogen) to obtain the seismic velocity (Ciz and Shapiro, 2007). The kerogen–oil mixture consists of oil bubbles embedded in a kerogen matrix and the clay mineral is transversely isotropic. Calculation of the Gassmann moduli requires knowing the dry-rock elastic constants. At the beginning of the maturation process (i.e., at 100% kerogen saturation), these can be obtained by using inverse Gassmann's equation or, alternatively, by the method developed by Ciz and Shapiro (2009) (see below).

3.1. Properties of the kerogen–oil mixture

The stiffnesses of the mixture can be calculated by using the model developed by Kuster and Toksöz's (1974). If s_o is the oil saturation, $s_o = \phi_o/(\phi_o = \phi_k)$, the stiffnesses are

$$\frac{K_{if}}{K_k} = \frac{1 + [4\mu_k(K_o - K_k)/(3K_o + 4\mu_k)K_k]s_o}{1-[3(K_o - K_k)/(3K_o + 4\mu_k)]s_o} \tag{20}$$

and

$$\frac{\mu_{if}}{\mu_k} = \frac{(1-s_o)(9K_k + 8\mu_k)}{9K_k + 8\mu_k + s_o(6K_k + 12\mu_k)}, \tag{21}$$

where $K_k = 1/c_k$ and $K_o = 1/c_o$. The density of the mixture is simply $\rho_{if} = (\phi_k\rho_k + \phi_o\rho_o)/(\phi_k + \phi_o)$.

3.2. Wet- and dry-rock Gassmann velocities

Ciz and Shapiro (2007) obtained the undrained compliance tensor when the pore infill and solid grains are anisotropic materials,

$$\bar{s}_{ijkl} = s^m_{ijkl} - \left(s^m_{ijmn} - s^s_{ijmn}\right)\left[\phi\left(s^{if} - s^{\phi}\right) + s^m - s^s\right]^{-1}_{mnqp}\left(s^m_{qpkl} - s^s_{qpkl}\right), \quad (22)$$

where the s's are the components of the compliance tensor, and the Einstein summation is assumed over 1, 2 and 3. Since the shale is transversely isotropic, the conversion between the Voigt stiffnesses and compliances and the 4th-rank tensors is

$$\begin{aligned} &s_{IJ} = s_{iijj},\\ &s_{II} = 4s_{ijij},\ i \neq j,\\ &c_{IJ} = c_{ijkl},\\ &I = i\delta_{ij} + \left(1-\delta_{ij}\right)(9-i-j),\\ &J = k\delta_{kl} + (1-\delta_{kl})(9-k-l), \end{aligned} \quad (23)$$

where δ_{ij} is the Kronecker delta, and no implicit summation is assumed. Note the symmetries $s_{ijkl} = s_{jikl} = s_{ijlk} = s_{klij}$ and similar relations for the stiffnesses (see Helbig, 1994). The relations between the Voigt stiffnesses and compliances are:

$$\begin{aligned} &c_{11} + c_{12} = s_{33}/s,\\ &2c_{66} = c_{11} - c_{12} = 1/(s_{11} - s_{12}),\\ &c_{13} = -s_{13}/s,\\ &c_{33} = (s_{11} + s_{12})/s,\\ &c_{55} = 1/s_{55},\\ &s = s_{33}(s_{11} + s_{12}) - 2s^2_{13}. \end{aligned} \quad (24)$$

The equations for the inversion are obtained by interchanging all c's and s's. The components of the corresponding undrained matrices transform in the same way.

In the case that the skeleton is made of a homogeneous material, $s^{\phi} = s^s$. In the limit of high porosities, say beyond 50%, the dry-rock elastic constants s^m_{ijkl} are zero in practice. In this limit, Eq. (22) becomes

$$\bar{s}_{ijkl} = (1-\phi)s^s_{ijkl} + \phi s^{if}_{ijkl}, \quad (25)$$

i.e., a generalization of the Reuss average.

In the isotropic case, the bulk modulus of the wet rock is given by the following Gassmann modulus

$$\overline{K} = K_m + \alpha^2 M, \alpha = 1 - \frac{K_m}{K_s}, M = \left(\frac{\alpha-\phi}{K_s} + \frac{\phi}{K_{if}}\right)^{-1}, \quad (26)$$

where K_s is the bulk modulus of the mineral grains and K_m is the dry-rock bulk modulus. A similar equation for the shear modulus is obtained by replacing K by μ.

Eq. (22) can be inverted to obtain the dry-rock compliance tensor as a function of the undrained compliance tensor. We have

$$s^m_{ijkl} = s^s_{ijkl} + \phi\left(\bar{s}_{ijmn} - s^s_{ijmn}\right)\left[\phi\left(s^{if} - s^{\phi}\right) - \bar{s} + s^s\right]^{-1}_{mnqp}\left(s^{if}_{qpkl} - s^{\phi}_{qpkl}\right). \quad (27)$$

This equation can be used to obtain the drained compliance tensor by using calibration data (seismic, well or laboratory data).

3.2.1. Mineral properties and dry-rock stiffnesses dependence on pressure

It is difficult to obtain the dry-rock stiffnesses for shale as a function of pore pressure, since a complete set of experimental data preserving the in-situ conditions is necessary. For instance, Ciz and Shapiro (2009) have recently obtained the stiffnesses for a North-Sea shale using a porosity-deformation approach. This theory assumes that the stress-dependent geometry of the compliant pore space controls the stress-induced variations. The components of the compliance tensor depend on exponential functions of the principal components of the effective stress tensor.

We use Eq. (27) to obtain the dry-rock stiffnesses from experimental data with 100% kerogen occupying the pore space, and assuming an exponential dependence on the differential pressure p_d,

$$c^m_{IJ} = \hat{c}_{IJ} + \check{c}_{IJ}\exp\left(-p_d/p^*_{IJ}\right), \quad (28)$$

where $p_d = p_c - p_H$, with p_c the confining pressure and p_H the hydrostatic pressure. In general, the confining pressure can be obtained by integrating the density log (as $\int g\bar{\rho}dz$). Here we assume $p_d = (\bar{\rho} - \rho_w)gz$. The parameters $\hat{c}_{IJ}$, $\check{c}_{IJ}$ and $p_{IJ}{}^*$ are obtained from the data using the stiffnesses at three different confining pressures and assuming an effective pressure law, i.e., replacing p_d by p_c (with $p_H = 0$) should give the same value of the elastic constants (e.g., Gei and Carcione, 2003). From the experimental data (e.g., Vernik and Nur, 1992), we have the sets $c^{(1)}_{IJ}$, $c^{(2)}_{IJ}$ and $c^{(3)}_{IJ}$, at p_{c1}, p_{c2} and p_{c3}, respectively. We obtain the unknown parameters from

$$\check{c}_{IJ} = \frac{c^{(3)}_{IJ} - c^{(1)}_{IJ}}{exp\left(-p_{c3}/P^*_{IJ}\right) - exp\left(-p_{c1}/p^*_{IJ}\right)}, \quad (29)$$

$$\hat{c}_{IJ} = c^{(1)}_{IJ} - \check{c}_{IJ}\, exp\left(-p_{c1}/p^*_{IJ}\right), \quad (30)$$

and

$$\left(c^{(3)}_{IJ} - c^{(1)}_{IJ}\right) exp\left[(p_{c1} + p_{c3})/p^*_{IJ}\right] + \left(c^{(1)}_{IJ} - c^{(2)}_{IJ}\right) exp\left[p_{c1} + p_{c2}/p^*_{IJ}\right] + \left(c^{(2)}_{IJ} - c^{(3)}_{IJ}\right) exp\left[p_{c2} + p_{c3}/p^*_{IJ}\right] = 0. \quad (31)$$

The dry-rock elastic constants should satisfy the conditions of physical stability. For a transversely isotropic medium these are

$$c^m_{11} > |c^m_{12}|,\ (c^m_{11} + c^m_{12})c^m_{33} > 2(c^m_{13})^2,\ c^m_{55} > 0 \quad (32)$$

(e.g., Carcione, 2007). The elastic constants of the mineral grains, c^s_{IJ}, are constrained by these conditions. We assume isotropy ($c^s_{11} = c^s_{33}$, $c^s_{66} = c^s_{55}$, $c^s_{12} = c^s_{13} = c^s_{11} - 2c^s_{66}$) and a Poisson medium ($c^s_{13} = c^s_{55}$) and then choose the medium with maximum stiffness satisfying Eq. (27).

3.3. Wet-rock velocities

The P and S seismic velocites are given by

$$\begin{aligned} &v_{33} = v_P(0) = \sqrt{\bar{c}_{33}/\rho},\\ &v_{11} = v_P(90) = \sqrt{\bar{c}_{11}/\rho},\\ &v_{55} = v_S(0) = \sqrt{\bar{c}_{55}/\rho},\\ &v_{66} = v_S(90) = \sqrt{\bar{c}_{66}/\rho}. \end{aligned} \quad (33)$$

where 0 and 90 correspond to the propagation angles perpendicular to and along the layering. Note that the qSV wave has the velocity $v_S(0)$ along these directions and the SH wave has the velocities $v_S(0)$ and $v_S(90)$, respectively.

The bulk density is given by

$$\rho = (1-\phi)\rho_s + \phi\rho_{if}. \quad (34)$$

4. Example

A typical source rock in the North Sea is represented by the Kimmeridge shale from the Draupne Formation, with a maximum thickness of nearly 200 m, overlain by a high-velocity chalk. The observed velocity contrast and thickness make the Kimmeridge an easily identified seismic unit.

We first verify that a single cracking reaction is a suitable approximation to model the kerogen/oil conversion. Thus, as Berg and Gangi (1999), we consider a single activation energy. Fig. 2a and b shows the concentration of kerogen $1-F$ as a function of temperature, corresponding to "J70 Upper Jurassic Kimmeridge Clay Formation" and Monterey shale, indicated as organofacies B and A, respectively, in Pepper and Corvi (1995). The symbols represent the real data and the solid line our calculations. The activation energy and infinite-temperature rate used in Fig. 2a are $E=27{,}800$ cal/mol and $A=10^{14}$/m.y., while the geothermal gradient is $G=25$ °C/km and the sedimentation rate is $S=0.04$ mm/y (Ebukanson and Kinghorn, 1990). According to Eq. (6) the heating rate is 1 °C/Ma. The surface temperature is 15 °C. For the Monterey shale, we have used $E=26{,}000$ cal/mol and a heating rate of 12.8 °C/Ma, as reported by Pepper and Corvi (1995). As can be appreciated, the agreement is satisfactory.

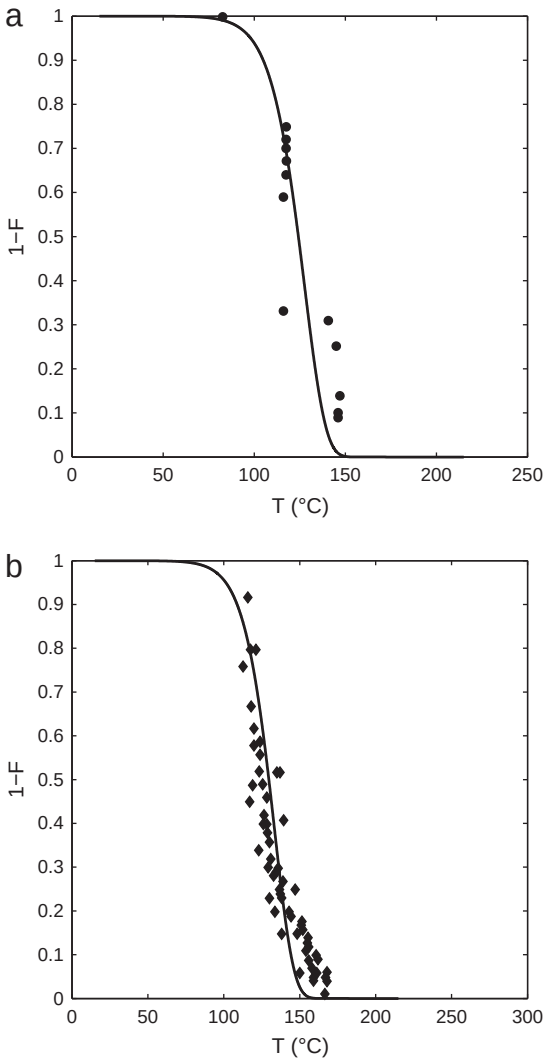

Fig. 2. Fraction of kerogen as a function of temperature for Kimmeridge shale (a) and Monterey shale (b). The solid lines correspond to our calculations using Eq. (4).

Next, we consider a sample fully saturated with kerogen, taken from a depth of 2768 m, whose velocities are given in Table 1 (see Tables A-1 and A-4 in Vernik (1995)).

The wet-rock elastic constants are given by

$$\begin{aligned}
&\bar{c}_{33}=\rho v_P^2(0),\\
&\bar{c}_{11}=\rho v_P^2(90),\\
&\bar{c}_{55}=\rho v_S^2(0),\\
&\bar{c}_{66}=\rho v_S^2(90),\\
&\bar{c}_{12}=2\bar{c}_{66}-\bar{c}_{11},\\
&\bar{c}_{13}=-\bar{c}_{55}+\sqrt{4\rho^2 v_P^4(45)-2\rho v_P^2(45)(\bar{c}_{11}+\bar{c}_{33}+2\bar{c}_{55})+(\bar{c}_{11}+\bar{c}_{55})(\bar{c}_{33}+\bar{c}_{55})},
\end{aligned} \tag{35}$$

(e.g., Carcione, 2007). Based on a grain density $\rho_s=2170$ kg/m^3 and kerogen properties $v_P=2600$ m/s, $v_S=1200$ m/s, $\rho_k=1400$ kg/m^3, the wet-rock elastic constants are given in Table 1. The properties of immature kerogen are obtained by fitting experimental data for the Kimmeridge shale provided by Vernik (1995). The kerogen content is K = 0.4 and the bulk density is $\rho=1862$ kg/m^3 (Vernik, 1995). The inversion using Eq. (27) yields the dry-rock elastic constants reported in Table 1. The elastic constants used for illite are $c_{33}^s=16.5$ GPa and $c_{55}^s=5.5$ GPa, corresponding to a Poisson medium with $v_P=2760$ m/s, $V_S=1593$ m/s and $\rho_s=2170$ kg/m^3. This choice satisfies the stability conditions (Eq. (32)). The clay in this shale is predominantly represented by illite and kaolinite, with the volume percent of smectite varying from 0 to 10% of the rock. The low velocities for illite may account for a fluid softening effect by hydration of the smectite. As can be seen in Table 1, the elastic constants c_{33}^m and c_{55}^m, related to the direction perpendicular to layering, are more affected by changes in the confining pressure, particularly c_{33}^m.

Using Eqs. (29), (30) and (31), we obtain

$$\begin{aligned}
&\hat{c}_{11}=19.72\ \text{GPa},\ \check{c}_{11}=-0.67\ \text{GPa},\ p_{11}^*=17.73\ \text{MPa},\\
&\hat{c}_{13}=5.54\ \text{GPa},\ \check{c}_{13}=-0.88\ \text{GPa},\ p_{11}^*=22.10\ \text{MPa},\\
&\hat{c}_{33}=15.98\ \text{GPa},\ \check{c}_{33}=-18.81\ \text{GPa},\ p_{33}^*=15.72\ \text{MPa},\\
&\hat{c}_{55}=4.40\ \text{GPa},\ \check{c}_{55}=-1.24\ \text{GPa},\ p_{55}^*=27.64\ \text{MPa},\\
&\hat{c}_{66}=6.87\ \text{GPa},\ \check{c}_{66}=-0.52\ \text{GPa},\ p_{66}^*=19.43\ \text{MPa}.
\end{aligned} \tag{36}$$

Typical pore space compressibilities range from $c_p=3\times10^{-6}$/psi (4.2×10^{-4}/MPa, rigid rock) to $c_p=30\times10^{-6}$/psi (42×10^{-4}/MPa, compliant rock), which correspond to incompressibilities of 2381 and 238 MPa, respectively. These values are in the range commonly measured for various types of rock (e.g., Fatt, 1958). As the porosity decreases, the pore space stiffness generally decreases, and therefore

Table 1
Properties of the source-rock.

p_c (MPa)	$v_P(0)$ (m/s)	$v_P(45)$ (m/s)	$v_P(90)$ (m/s)	$v_S(0)$ (m/s)	$v_S(90)$ (m/s)
5	2690	2890	3520	1490	1910
30	2820	3030	3680	1540	1990
70	2920	3150	3790	1570	2020

p_c (MPa)	$\bar{c}_{11}$ (GPa)	$\bar{c}_{33}$ (GPa)	$\bar{c}_{13}$ (GPa)	$\bar{c}_{55}$ (GPa)	$\bar{c}_{66}$ (GPa)
5	23.1	13.5	3.1	4.1	6.8
30	25.2	14.8	3.8	4.4	7.4
70	26.8	15.9	5	4.6	7.6

p_c (MPa)	c_{11}^m (GPa)	c_{33}^m (GPa)	c_{13}^m (GPa)	c_{55}^m (GPa)	c_{66}^m (GPa)
5	19.2	2.3	4.8	3.3	6.5
30	19.6	13.1	5.3	4	6.8
70	19.7	15.8	5.5	4.3	6.9

c_p increases. Following Mavko and Mukerji (1995) and neglecting the mineral grain compressibility (see Eq. (8) in Zimmerman et al., 1986), we consider that the pore space stiffness c_p^{-1} decreases linearly with porosity (kerogen content). We assume

$$c_p\left[\mathrm{MPa}^{-1}\right] = (2381-5357\mathrm{K})^{-1}, \tag{37}$$

such that the pore space stiffness lies between the upper and lower limits mentioned above: 2381 MPa for $K\approx 0$, and 238 for $K=0.4$. As for sandstones, Eq. (37) is based on the "critical porosity" concept. The critical porosity K_c separates load-bearing sediments from suspensions (in this case $K_c\approx 0.44$ for $c_p=\infty$). According to Eq. (37), a Kimmeridge shale with 35% kerogen content has a pore stiffness of 506 MPa.

Fig. 3 shows the fraction of kerogen converted to oil as a function of depth for two sedimentation rates, three different geothermal gradients and an activation energy $E=25{,}000$ cal/mol (Berg and Gangi, 1999; Connan, 1974). At a given depth, the conversion increases with increasing geothermal gradient and decreasing sedimentation rate. We show the plots till a depth corresponding to the fracture pressure, which is assumed to be 0.94 p_c. Beyond this point, the physics described by the equations given in this work is not anymore valid.

Let us consider in the following a geothermal gradient $G=25$ °C/km and a sedimentation rate $S=0.08$ mm/y. The oil properties are assumed to be $v_P=730$ m/s, $v_S=0$, $\rho_o=900$ kg/m^3 (McCain, 1984). Moreover, $\overline{\rho}=2.5$ g/cm^3 and $\rho_w=1.04$ g/cm^3. The porosity and the kerogen and oil fractions versus depth are represented in Fig. 4. As can be seen the porosity increases with depth; the equation $\phi=\phi_k+\phi_o$ is satisfied.

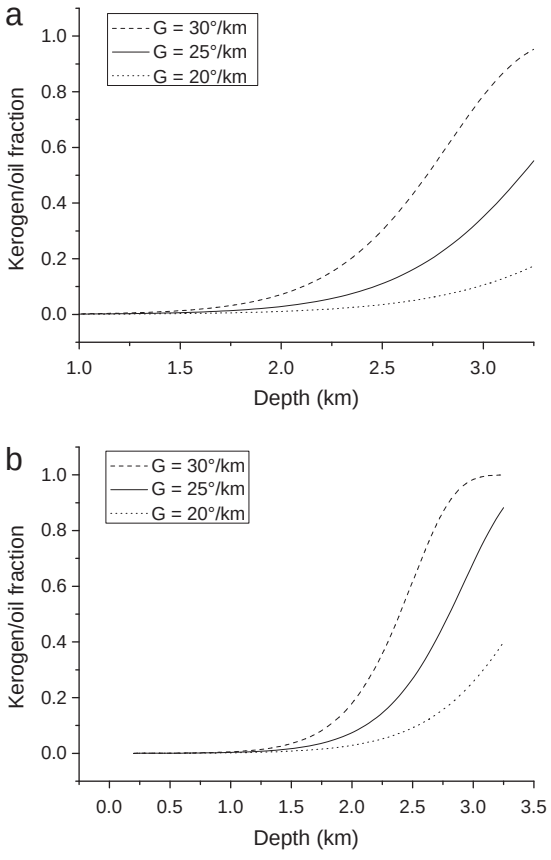

Fig. 3. Fraction of kerogen converted to oil (F) as a function of the depth for sedimentation rates $S=0.08$ km/yr (a) and $S=0.03$ km/yr (b), and three different geothermal gradients.

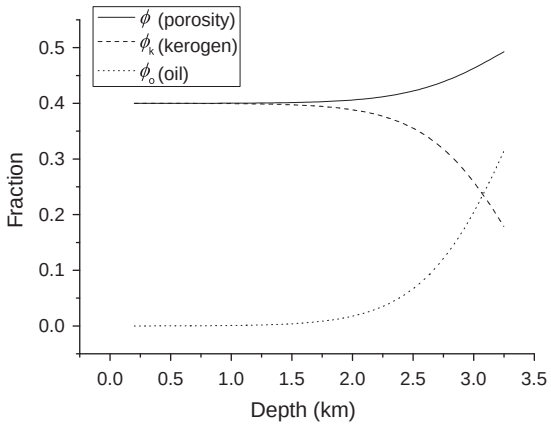

Fig. 4. Porosity and kerogen and oil fractions as a function of depth.

"Creation of porosity" has been reported by Goff (1983), who analyzed the hydrocarbon generation and migration from Jurassic source rocks of North-Sea basins, in particular he obtained the change in porosity during maturation of the Kimmeridge–Clay source rock, with 30% oil expulsion (his Table 7), and showed that the total porosity at first decreases as water is expelled from the rock, but then increases slightly near peak oil generation. He states "oil saturation in the effective porosity of the rock (comprising the abnormally large rock matrix pores and porosity in the kerogen laminae) increases from 35% at a transformation ratio of 0.1, to 55% at quarter generation". As mentioned above, in our calculations the fluid is not allowed to be expelled from the source rock and the porosity increase is overestimated by a given amount, but in qualitative terms our model is able to reproduce the physics of the conversion.

The pore pressure is shown in Fig. 5 and the velocities in Fig. 6. As expected, the horizontal velocities are greater than the vertical velocities and the degree of anisotropy increases with depth. The vertical P-wave velocity decreases almost by 1 km/s from the surface to the depth of fracture, being the principal indicator of overpressure. The other velocities remain nearly constant from a practical point of view.

5. Conclusions

We have performed a simple analytical basin modeling, based on constant geothermal and geodynamic properties, to obtain the fraction of kerogen converted to oil and pore pressure in a source

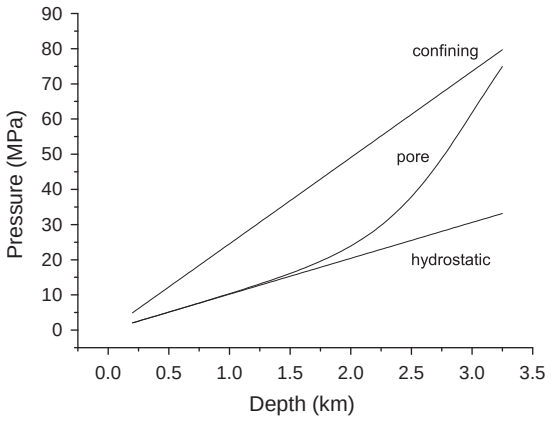

Fig. 5. Hydrostatic, pore and confining pressures as a function of depth.

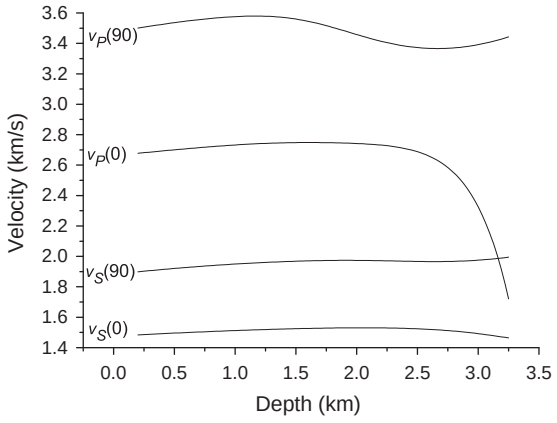

Fig. 6. P- and S-wave velocities as a function of depth, along the horizontal (90) and vertical (0) directions.

rock subject to a uniform sedimentation rate. Gassmann's equations for an anisotropic frame and an isotropic solid pore infill (kerogen–oil) allows us to obtain the seismic velocities till the depth of fracture. The effective properties of illite are obtained by assuming an isotropic Poisson medium constrained by the physical stability conditions applied to the elastic constants of the dry frame, which are obtained by inversion of Gassmann's equations. The method is applied to the Kimmeridge shale and shows that the vertical P-wave velocity is the main indicator of overpressure, varying by almost 40% the value at normal pressure conditions.

Acknowledgment

We thank Anthony Gangi for useful suggestions.

References

Berg, R.R., Gangi, A.F., 1999. Primary migration by oil-generation microfracturing in low-permeability source rocks: application to the Austin Chalk, Texas. AAPG Bull. 83 (5), 727–756.
Carcione, J.M., 2000. A model for seismic velocity and attenuation in petroleum source rocks. Geophysics 65, 1080–1092.
Carcione, J.M., 2007. Wave fields in real media, Theory and Numerical Simulation of Wave Propagation in Anisotropic, Anelastic, Porous and Electromagnetic Media, 2nd edition. Elsevier Science. revised and extended.
Carcione, J.M., Gangi, A., 2000a. Non-equilibrium compaction and abnormal pore-fluid pressures: effects on seismic attributes. Geophysical Prospecting 48, 521–537.
Carcione, J.M., Gangi, A., 2000b. Gas generation and overpressure: effects on seismic attributes. Geophysics 65, 1769–1779.
Ciz, R., Shapiro, S., 2007. Generalization of Gassmann equations for porous media saturated with a solid material. Geophysics 72, A75–A79.
Ciz, R., Shapiro, S., 2009. Stress-dependent anisotropy in transversely isotropic rocks: comparison between theory and laboratory experiment on shale. Geophysics 74, D7–D12.
Connan, J., 1974. Time–temperature relationship in oil genesis. AAPG Bull. 58, 2518–2521.
Das, A., Batzle, M., 2008. Modeling studies of heavy oil — in between solid and fluid properties. The Leading Edge 1116–1123 September.
Ebukanson, E.J., Kinghorn, R.R.F., 1990. Jurassic mudrock formations of southern England: lithology, sedimentation rates and organic carbon content. Journal of Petroleum Geology 13, 221–228.
Fatt, I., 1958. Pore volume compressibilities of sandstone reservoir rocks. AIME Petroleum Transactions 213, 362–364.
Gautschi, W., Cahill, W.F., 1964. Exponential integral and related functions. In: Abramowitz, M., Stegun, I.A. (Eds.), Handbook of Mathematical Functions with Formulas, Graphs and Mathematical Tables. : Applied Math. Series, 55. U. S. Department of Commerce, National Bureau of Standars, Washington, D. C, pp. 227–254. S5.
Gei, D., Carcione, J.M., 2003. Acoustic properties of sediments saturated with gas hydrate, free gas and water. Geophysical Prospecting 51, 141–157.
Goff, J.C., 1983. Hydrocarbon generation and migration from Jurassic source rocks in the E Shetland Basin and Viking Graben of the northern North Sea. J. Geol. Soc. London 140, 445–474.
Helbig, K., 1994. Foundations of Anisotropy for Exploration Seismics. Pergamon Press.
Kuster, G.T., Toksöz, M.N., 1974. Velocity and attenuation of seismic waves in two-phase media: part I. Theoretical formulations, Geophysics 39, 587–606.
Luo, X., Vasseur, G., 1996. Geopressuring mechanism of organic matter cracking: numerical modeling. AAPG Bulletin 80, 856–874.
Mavko, G., Mukerji, T., 1995. Seismic pore space compressibility and Gassmanns relation. Geophysics 60, 1743–1749.
McCain Jr., W.D., 1984. The Properties of Petroleum Fluids. PennWell Books, Tulsa, OK.
Pepper, A.S., Corvi, P.J., 1995. Simple kinetic models of petroleum formation. Part I: oil and gas generation from kerogen. Marine and Petroleum Geology 12, 291–319.
Vernik, L., 1995. Petrophysics of the Kimmeridge Shale. Stanford Rock Physics Laboratory, North Sea.
Vernik, L., 1994. Hydrocarbon-generation-induced microcracking of source rocks. Geophysics 59, 555–563.
Vernik, L., Landis, C., 1996. Elastic anisotropy of source rocks: implications for hydrocarbon generation and primary migration. AAPG Bulletin 80, 531–544.
Vernik, L., Nur, A., 1992. Ultrasonic velocity and anisotropy of hydrocarbon source rocks. Geophysics 57, 727–735.
Zimmerman, R.W., Somerton, W.H., King, M.S., 1986. Compressibility of porous rocks. Journal of Geophysical Research 91, 12765–12777.